Research Paper

Assessing the Sensitivity of Seismic Loss Estimation to the Geographic Resolution of Building Exposure Model

Nazila Kheirkhah[1], Mohsen Kalantari[2], Erfan Firuzi[3*] and Kambod Amini-Hosseini[4]

1. M.Sc. Degree, Institute of Geophysics, University of Tehran, Tehran, Iran
2. M.Sc. Degree, K.N. Toosi University of Technology, Tehran, Iran
3. Ph.D. Degree, International Institute of Earthquake Engineering and Seismology (IIEES), Tehran, Iran, *Corresponding Author; email: e.firuzi@iiees.ac.ir
4. Associate Professor, Risk Management Research Center, International Institute of Earthquake Engineering and Seismology (IIEES), Tehran, Iran

Received: 08/11/2022
Revised: 10/01/2023
Accepted: 28/01/2023

ABSTRACT

This paper assessed the sensitivity of seismic losses to the geographic resolution of building exposure model. One of the key steps of seismic risk assessment is providing an accurate and reliable building inventory. Generally, building exposure model is derived from various sources of information with different degrees of quality and accuracy. Therefore, compilation of exposure model is a complex process that is associated with uncertainties. In this regard, selecting the most appropriate geographic resolution of building exposure model is a challenge. There is a trade-off between the accuracy of ground motion values in the centroid of grid cells and computation efficiency. On the one hand, selecting a higher resolution will result in less efficient computing. Increased grid cell size, on the other hand, will impose uncertainty on the results due to inaccuracy in estimating ground motion values in the proper location of buildings. The purpose of this study is to address this question "what is the impact of geographic resolution of exposure model on the seismic risk assessment?" To do so, a sensitivity analysis with three distinct levels of resolution was performed in Tehran, Iran, as a case study, to evaluate the impact of exposure model resolution on estimated losses. The results showed that total damage over the region is almost insensitive to the resolution of exposure models; while, a more accurate damage map with lower standard deviation is achieved by refining resolutions. This is an important outcome that will assist researchers performing seismic risk assessment in large geographic areas, like countries or provinces, to be aware of the effects of geographic resolution of exposure model on results.

Keywords:
Exposure Model;
Geographic Resolution;
Seismic risk assessment;
Uncertainty; Tehran

1. Introduction

Proper estimation of seismic damage, economic and human losses from a possible future earthquake is an important subject to national authorities, regional governments, financial institutions, insurance and reinsurance industries. Such studies provide the key information for decision makers to take proper steps towards risk mitigation actions. The basic three components of seismic risk assessment are: 1) seismic hazard, 2) exposure model and 3) fragility or vulnerability models [1]. The seismic hazard provides information regarding the surface ground motion shaking values in the region of interest. The term "exposure" refers to any element at risk including buildings, population and life-line systems. The main concentration of this study is building exposure model. Building exposure model generally contains information like the location, structural characteristics, built-area, content value of buildings at risk. The third component of seismic damage and loss estimation are fragility or vulnerability curves. The vulnerability curves express the ratio of loss to the total exposed economic value; while, fragility curves describe the probability of exceeding a certain damage state threshold from a given ground motion level [2].

Each of the aforementioned components is associated with uncertainties that should be identified, quantified and incorporated in calculation effectively. Crowley [3] provides a comprehensive discussion regarding the uncertainties of risk assessment. According to Crowley [3], exposure is typically derived from poor data with a large number of assumptions, and is arguably the most uncertain component of risk assessment. The report published by Organization for Economic Cooperation and Development (OECD) [4] also indicated that exposure model is an important factor in seismic risk assessment and associated with uncertainty that should be modelled properly [5]. All aforementioned studies highlighted the key role of exposure model in seismic risk assessment. Despite the key role of exposure model on seismic risk assessment, the exposure model is rarely considered as an uncertain parameter in practice. Generally, exposure models suffer from incomple-teness (lack of proper information) and inaccuracies (uncertainties in their exact location). In the common practice of seismic risk assessment, the building inventories are typically modelled as aggregated within administrative units or grid cells. Even, in the case of accessing an ideal database (i.e., building by building) for computational efficiency (particularly in case of a large-scale region), the exposure database is often modelled as aggregated within grid cells. Clearly, this aggregation will impose uncertainties on the results. Most of this uncertainty stems from inaccuracies for estimating the ground motion values in grid cells (a coarser resolution of grid cells imposes higher uncertainties on ground motion values due to ambiguity in estimating distance of site from epicenter).

The above issue has been discussed in few studies in a quantitively manner. Bazzurro and Park [6] indicated that aggregating building portfolio at the zip code level leads to an under-estimation of losses in low return period. Similar conclusion was also provided by Bal et al. [7] and Scheingraber and Kaser [8]. Bal et al. [7] assessed the impact of geographic resolution of exposure model on seismic losses in four distinct geo-resolution levels. Their results showed that the average total damage over the region is almost insensitive to the resolution of exposure models; while, a more accurate damage map with lower standard deviation is achieved by refining resolutions. Dabeek et al. [9] also evaluated the impact of exposure model on seismic losses, in terms of Annualized Earthquake Loss (AEL), in 35 countries of Europe. Their results indicated that the value of AEL will may leads to a bias of 27% in different geo-resolutions of exposure model. They stated that keeping the spatial resolution of exposure under 240 arc-second leads a bias of less than 5%.

By considering the aforementioned explanations, this study assessed the impact of geographic resolution of exposure model on seismic risk assessments in Tehran, Iran. Generally, the building exposure model in Iran is derived from information provided by Statistical Center of Iran (SCI) [10]. This is the official center for compiling information regarding the buildings and population in Iran. SCI [10] provides information in census blocks (the highest available geographic resolution). However, in many large-scale studies, such as countries and provinces, researchers used a coarser resolution of exposure model. This simplification is employed for increasing the computation efficiency. As a case in point, Motamed et al. [11] performed a seismic risk assessment with an exposure model with grid-cells size of 10 km × 10 km for whole of Iran, which is significantly lower than available information provided SCI [10]. Similarly, Mansouri et al. [12], as a part of GEM-EMME project, developed a residential and population database of Iran in grid cells of 5km × 5km. Shahbazi et al. [13] also developed a buildings inventory by resolution of 1 km × 1km for entire Iran for introducing a loss transfer functions to model seismic financial loss. To assess the impact of these varied geographic resolutions on seismic risk assessment, in the present study, a sensitivity analysis is performed.

In following sections, first, a discussion about available uncertainties regarding the geographic resolution of exposure model was represented. Then, a sensitivity analysis was performed to evaluate the impact of exposure model resolution on seismic risk in Tehran, capital of Iran, as a case study. To do so, the losses, in terms of mean damage ratio, in three distinct levels of exposure model resolution were estimated for the Ray fault seismic scenario (6.7 Mw) and results are compared. In conclusion, a comprehensive discussion regarding the results and influence of exposure resolution on seismic risk assessment were presented.

2. Uncertainties of Building Exposure Model in Seismic Risk Assessment

Development of a reliable building exposure model will improve the estimation of seismic risk assessment. This is an important step that involved several simplifications and uncertainties. Alongside the uncertainty due to the incompleteness and inaccuracy, in the case of aggregated exposure model, the spatial resolution of exposure model imposes uncertainties on results. Thus, selecting appropriate size of grid cells is an important issue in developing of exposure database. This parameter has a direct impact in both accuracy and computational efficiency. In fact, there is a trade-off between the accuracy of seismic risk assessment and computational efficiency. On the one hand, selecting a finer grid cell with higher resolution will reduce the computation efficiency. On the other hand, increasing the size of grid cell will impose uncertainties on the results from inaccuracy of ground motion shaking values within the grid cell as the representative the distribution of building inventories within the grid cells.

In the aggregated exposure model, generally, the ground motion value of a single point within the grid cell or administrative unit is used as input to the fragility and vulnerability models. Accordingly, this approach cannot capture the inherent spatial correlation of ground motion shaking in the smaller scale geo-resolution. That is, for all assets in the grid cell the same sample of GMPEs uncertainty is implemented, this means that there is a full spatial correlation of ground motion shacking for all assets in the grid cell; while in reality each asset will subjected to the different ground motion shacking [3, 6]. In addition, selecting the most appropriate point within the grid cells or administrative unit that is a representative of the distribution of assets within the grids is a challenging issue. Generally, it is assumed that the assets are uniformly distributed within the grid cell and the centroid of the grid cells is used for estimation of ground motion shacking. While in the case of a very unbalanced distribution of building inventories this simplified assumption may impose a significant error to the loss estimations [7, 14]. It should be noticed, if the number of assets and their corresponding distribution within the grid cells are available, a random sampling of the points based on the probability distributions of assets and random sampling of variability of ground motion shacking can be proposed as an effective approach in handling of the aforementioned uncertainties. Although this approach increase significantly the computational demands when the number of assets are large.

This study investigates the influence of exposure resolution on the result of seismic risk assessment. To this end, Tehran, Iran's capital is used as a case study. The seismic loss is assessed for three distinct levels of resolution including, grid cells with size of 1 km × 1 km, 3 km × 3 km and 5 km × 5 km. A schematic distribution of different sizes of grid cells is depicted in Figure (1). These grid sizes are selected by author based on the available information (the highest available information is census blocks which are generally in size one km^2) and considering the dimensions of the Tehran (the lowest geographic resolution in generally used for seismic risk assessment of the country).

3. Case Study Tehran

According to the recent data provided by SCI, Tehran has a population around 8.8 million (2016). This is the most populated and influential city of the Iran where most of political, economic and cultural centers are located. The rapid growth of the city leads to high concertation of population, construction and infrastructure in the region.

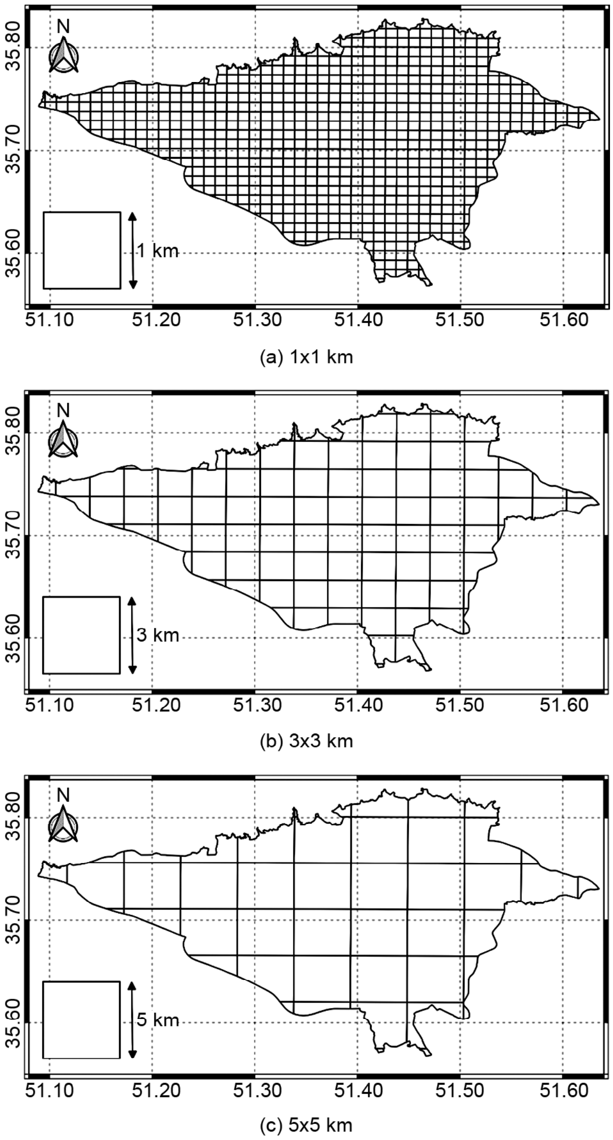

Figure 1. Three distinct levels of geospatial resolutions of compiled exposure models in Tehran.

Therefore, the safety of the city is important for the government. Tectonically, Tehran located in the southern edge of Alborz Mountain which is characterized by large earthquakes [15]. North Tehran Fault (NTF), Mosha, Ray and Taleghan are the most important seismic active sources in this region. Distribution of these seismic sources in relation to Tehran is demonstrated in Figure (2). Alongside, the high seismicity of the region, the high vulnerability of built environment also intensifies the seismic risk of region. This issue indicated in several studies [1, 16-18]. In a study done by JICA [16] the potential losses of Tehran in three distinct seismic scenarios including the rupture of Mosha, NTF and Ray is evaluated. Their results indicated that the Ray seismic scenario with 55% building damage ratio and 383,000 fatalities is the most vulnerable seismic scenario. In a similar analysis performed by Mansouri et al. [19], the rupture of Ray fault has the potential of producing 68% damages to residential buildings the Tehran. In that study, it was noticed that Ray fault has a significant potential of damages and losses in the southern part of Tehran which is densely populated region with many old masonry structures. In the present study, we select the same seismic scenario for performing the sensitivity analysis. In following subsections, the seismic hazard, exposure model and potential damages in Tehran for three distinct levels of resolution is presented.

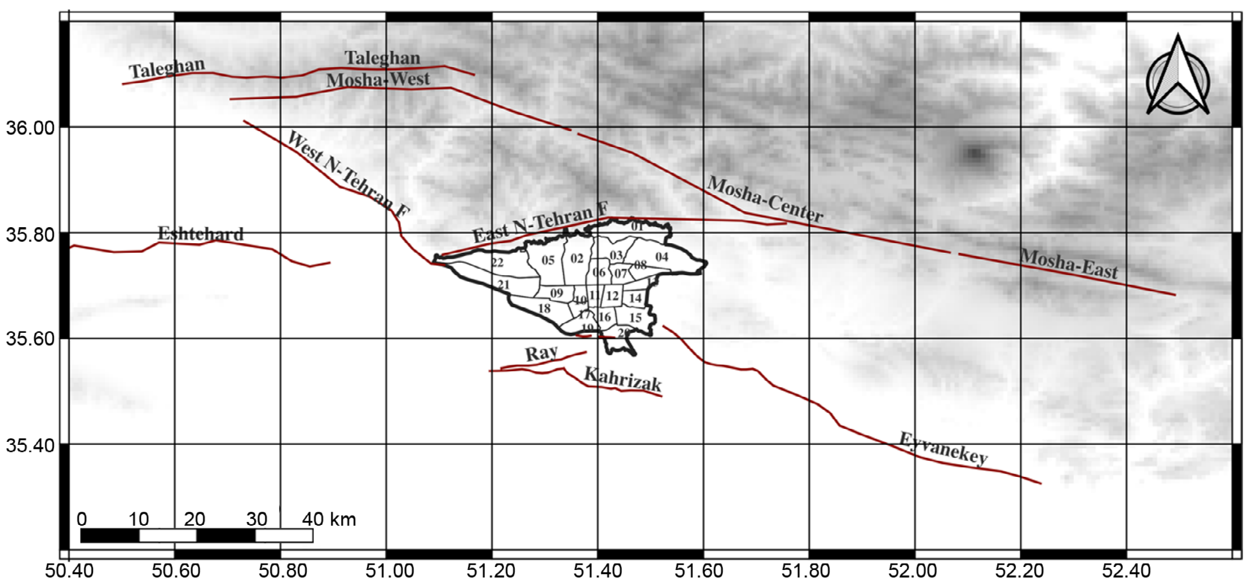

Figure 2. Distribution of active faults in relation to Tehran Boundaries (numbers are 22 municipal districts of Tehran); fault traces are taken from Hessami et al. [20].

3.1. Seismic Hazard Assessment for Ray Seismic Scenario

The Ray fault has two main segments: 1) north and 2) south Ray segments. In many studies, like Moinfar et al. [21], it is believed that that the root of north and south ray faults is the same and these are branches of one fault, so in the present study, a line representative fault model of both faults is considered in analysis. Summary of the most important model parameters are listed in Table (1). To generate the ground motion shacking map from the rupture of Ray fault, the OpenQuake program is used. This is an appropriate tool to incorporate the available uncertainties in seismic hazard assessment [22]. The uncertainty regarding the epicenter is considered in analysis through a random sampling from the fault trace. The iteration is performed 1,000 times. The magnitude of seismic scenario is considered 6.6 (Mw). This is in accordance with the relation of Wells and Coppersmith [23] which estimates the potential magnitude of a seismic source based on the length of fault. To take into account the epistemic uncertainties of Ground Motion Prediction Equations (GMPEs) the logic tree is employed. In the present study, five GMPEs of Kale et al. [24], Kotha et al. [25], Akkar and Bommer [26], Zhao et al. [27] and Idriss [28] are used. These relations showed good performance in the statistical tests performed by Firuzi et al. [2]. It should be mentioned that the intra-event uncertainty of GMPEs is incorporated in calculation by adding a random coefficients of intra-event variability (sigma) of GMPEs to logarithm of median value. The random sampling is carried out by considering the spatial correlation. The impact of spatial correlation on seismic risk assessment is demonstrated in several studies [29-30]. Here, the spatial correlation model proposed by Zafarani et al. [31] is used. This random sampling is also repeated 1,000 times. For deriving the surface ground motion values, the V_{S30} data is required. In the present study, the information provided by JICA [16] is used. JICA [16] by compiling data of boreholes introduced 41 soil types in Tehran. They also provided the amplification factor of different soil types. In this study, the same information is employed for considering the soil condition.

The surface ground motion values for one realization in different resolution levels are presented in Figure (3). As depicted, in all geo-resolution the ground motion values in the southern parts of the city, nearby the Ray fault, are higher. The results show that the PGA values in Tehran varies between 0.1 g to 0.65 g. The results are in agreement with ground motion shaking maps provided by JICA [16] and Mansouri et al. [19]. As depicted in Figure (3), by increasing the size of grid-cells the ground motion values are coarser and their corresponding spatial correlation is decreased. For-example, 25 grid-cells of the smallest resolution constitute one grid-cell of the lowest resolution. Thus, distribution of ground motion values in smaller geo-resolution is more accurate. Consequently, more accurate damage estimation is derived. This is achieved in the cost of high computation burden.

3.2. Compiling Exposure Model and Selecting Fragility Curves

For assessing the possible damages to building inventories a reliable exposure model and a set of compatible fragility curve are required. In the present study, the exposure model is derived from data provided by SCI on 2016. SCI is the most important source of information about population and building inventories in Iran. This center represents the information about the construction material, age of structure, built-in area, and population. Based on the data of SCI, the number of residential dwellings in Tehran is around 2,500,000 which cover a wide range of construction types with different quality and height. This heterogonous in construction types, quality and height make the classification scheme a challenge. Here, the building

Table 1. Summary of important model parameters for the Ray fault seismic scenario.

Parameter	Value	Reference
Strike, Dip	263°, 75°	Zafarani et al. [32]
Magnitude	6.7 (Mw)	Zafarani et al. [32]
Fault Dimension Along Strike and Dip	29, 14 (Km)	Wells and Coppersmith [23]
Depth	12 Km	-

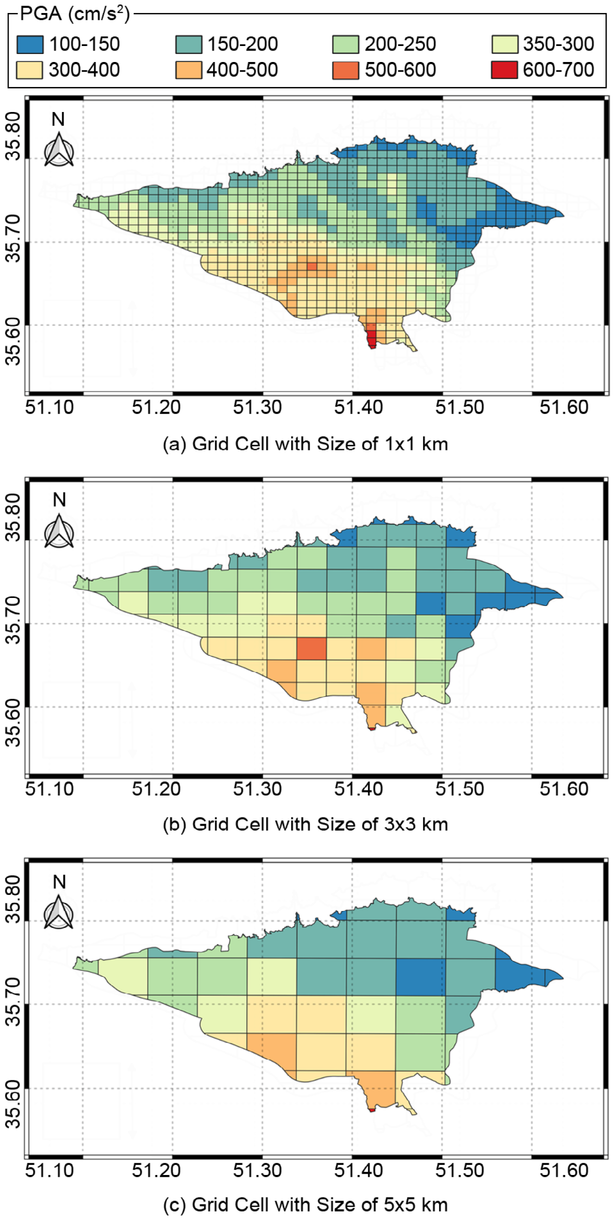

Figure 3. Distribution of PGA within three distinct levels of geo-resolution.

inventories are classified into various classes based on construction material, building quality and height.

Based on the construction material building inventories are categorized into three groups: 1) Reinforced-concrete 2) Steel and 3) Masonry. For simplicity, all adobe, masonry, rubble stone and other types of structures are placed into masonry class. It should be noticed that classification scheme is done according to the available census information. The year of the construction is used as the second index of classification. The year of construction is related to the corresponding seismic code used for designing building. The initial seismic regulation of structures in Iran is provided in a chapter of Iran's standard No. 519 in 1966. This provision contains the minimum load requirement on buildings and some technical constructions. In 1987, the first edition of a new and much more demanding design code under the title of "Iranian Code of Practice for Seismic Resistant Design of Building (Standard 2800)" is represented. The subsequent editions of this standard with more rigorous regulation are represented in 1996 (the second edition), 2005 (the third edition) and 2015 (the fourth edition). Based on the above explanations, buildings can be classified into three groups. Buildings constructed before the year 1986, between the years 1986 and 2006 and after the year 2006 are considered as low-code, mid-code and high-code, respectively. Distribution of dwelling based on the year of construction and construction material is shown in Figure (4). As it is clear, the quality of buildings has been changing during the past 30 years in Iran which is moving from non-engineering old masonry buildings to the engineering ones.

Building height is used as the last criteria of building classification. Regarding the number of stories, building classified into three groups. The low-rise building (with 1-3 stories), mid-rise building (with 4-6 stories) and high-rise building (with more than 7 stories). This information is added to the classification from additional database provided by Tehran municipal. Based on the aforementioned classification scheme, the building inventories are classified into 19 taxonomies, as presented in Table (2). Figure (5) shows distribution of buildings within different grid cells sizes in Tehran.

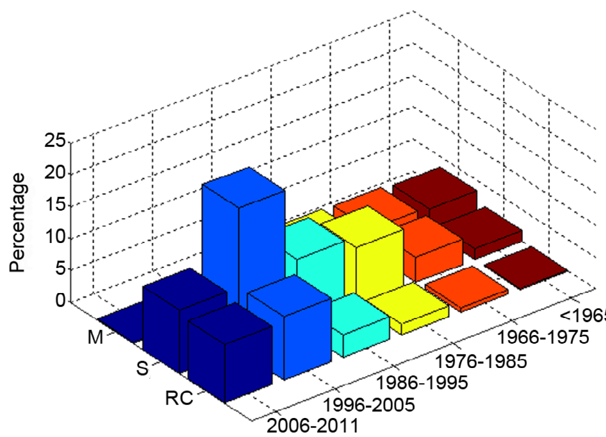

Figure 4. Distribution of dwelling according to the year of construction and structural type (M, S and RC are acronyms for Masonry, Steel and Reinforced-Concrete structures, respectively).

As depicted, there is a concentration of buildings in the middle and southern parts of Tehran, where is generally the home of low-income people. It should be emphasized once more that aggregating the buildings at a lower geo-resolution introduces ambiguity in the representation of the best point within

Table 2. The list of all building classes used in the present study.

No.	Class ID	Construction Type	Quality	Height
1	SLL	Steel	Low-Quality before 1986	Low-Rise (1-3 Stories)
2	SLM			Mid-Rise (4-6 Stories)
3	SLH			High-Rise (More Than 6)
4	SML		Mid-Quality between 1986 and 2006	Low-Rise (1-3 Stories)
5	SMM			Mid-Rise (4-6 Stories)
6	SMH			High-Rise (More Than 6)
7	SHL		High-Quality after 2006	Low-Rise (1-3 Stories)
8	SHM			Mid-Rise (4-6 Stories)
9	SHH			High-Rise (More Than 6)
10	RCLL	Reinforced Concrete	Low-Quality before 1986	Low-Rise (1-3 Stories)
11	RCLM			Mid-Rise (4-6 Stories)
12	RCLH			High-Rise (More Than 6)
13	RCML		Mid-Quality between 1986 and 2006	Low-Rise (1-3 Stories)
14	RCMM			Mid-Rise (4-6 Stories)
15	RCMH			High-Rise (More Than 6)
16	RCHL		High-Quality after 2006	Low-Rise (1-3 Stories)
17	RCHM			Mid-Rise (4-6 Stories)
18	RCHH			High-Rise (More Than 6)
19	M	Masonry	All	All

* The first character in the class id is representative of structure (M: Masonry, S: Steel, RC: Reinforced Concrete) the second character refers to the quality of construction (L: Low-quality, M: Mid-quality, H: High-quality), and the third character presents building height (L: Low-rise, M: Mid-rise, H: High-rise)

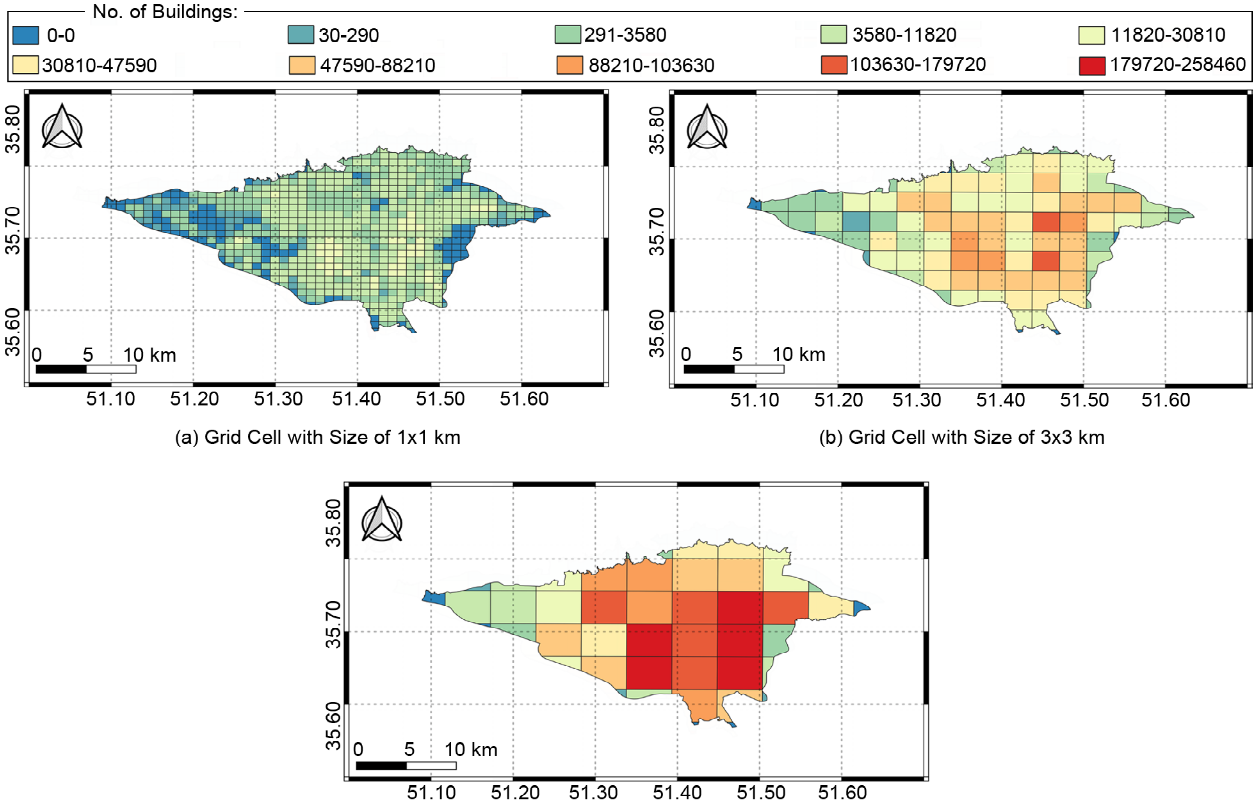

Figure 5. Distribution of dwelling within three distinct levels of geographic resolution.

the grid-cells for estimating ground motion values.

For providing a relation between the ground motion shaking and the probability of exceeding various damage states a set of fragility curve is required. Fragility curve is an important component of seismic risk assessment that should be compatible with pre-defined building classes. In the literature, there are a number of local fragility curves for typical buildings in Iran [16, 33-34]. Here, the fragility curves developed by Fallah-Tafti [33] are used. Fallah-Tafti [33] by collecting a set of existing fragility curves and combination of them based on the Analytic Hierarchy Approach (AHP) developed fragility curves with four damage states (slight, moderate extensive and complete). The main motivation for employing the proposed fragility curves of Fallah-Tafti [33] is consistent their taxonomy with buildings classification scheme used in this study.

3.3. Seismic Risk Assessment

This section provides the results of seismic risk, in terms of mean damage ratio, for three distinct levels of resolution. The analysis is performed using the OpenQuake software. This is an open-source and computationally efficient tool for seismic hazard and risk assessment [35]. The scenario damage calculator of OpenQuake computes probability of different damage states using the fragility curves. In the present study, the mean damage ratio is used for presenting the distribution of damages throughout the city. The mean damage ratio (MDR) is derived from Equation (1).

$$DR_i = \left(N_{s_i} \times DR_s + N_{m_i} \times DR_m + N_{e_i} \times DR_e + N_{c_i} \times DR_c\right) / N_{T_i} \qquad (1)$$

Where the N_{T_i} is the total number of dwellings in the ith grid cell. N_{s_i}, N_{m_i}, N_{e_i} and N_{c_i} are the number of dwelling in each grid cell in damage states of slight, moderate, extensive and collapse, respectively. DR_s, DR_m, DR_e and DR_c are corresponding mean damage factor for each damage state. The definition of damage states is compatible with HAZUS [35]. In Table (3) the range of damage factor for each damage state with their corres- ponding central value is represented.

Figure (6) shows the distribution of MDR throughout Tehran in three distinct levels of resolution. As depicted, most of damage is occurred in the southern and central parts of the city which are near the Ray fault. Figure (6) also shows that by

Table 3. The range of damage factor with their corresponding central value.

Damage State	Range of Damage Factor (%)	Mean Damage Factor (%)
None	0	0
Slight	0-4	2
Moderate	4-16	10
Extensive	16-84	50
Collapse	100	100

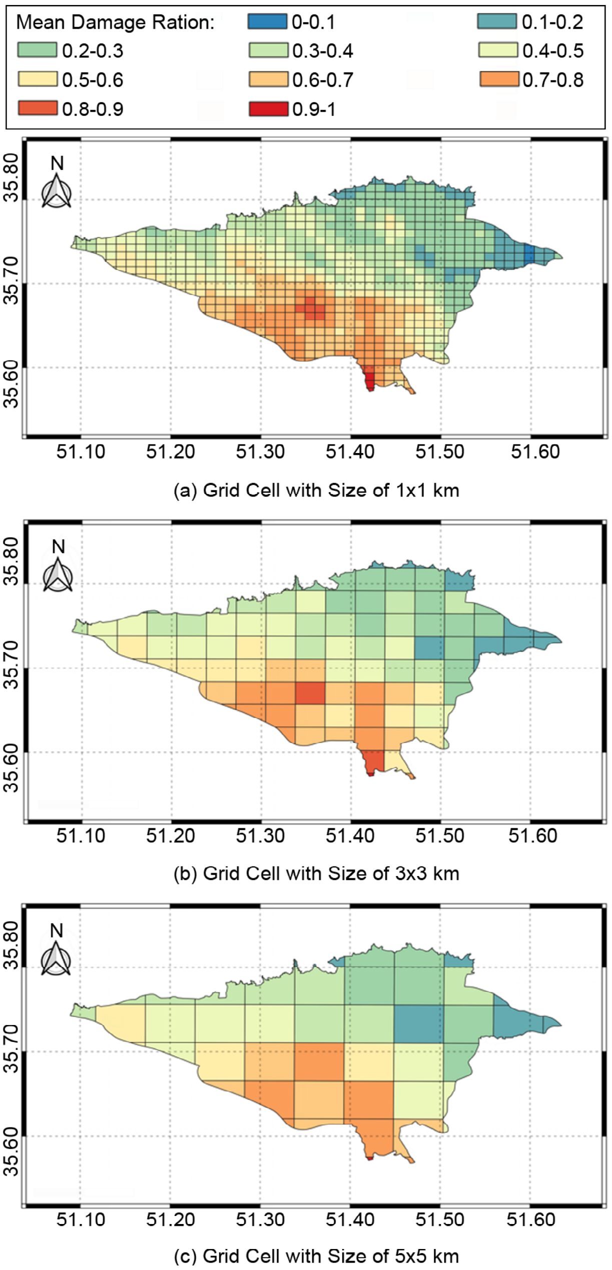

Figure 6. Distribution of mean damage ratio (MDR) throughout of the region by considering different resolution of exposure model.

moving towards a smaller resolution, the uncertainty due to using assumption of uniform distribution of assets in the grid cells and employing the centroid of grid cell as representative of grid for loss estimation will be reduced. Thus, more accurate results are obtained. In the case of a very unbalanced distribution of assets in a large-scale grid cells the implementing of centroid of grid cell may impose a significant error to the results [7].

In other to evaluate the influence of resolution of exposure model on total loss, the distribution of MDR for the whole of Tehran from 1,000,000 iteration of ground motion values and epicenters is shown in Figure (7). As depicted, the average of MDR is almost insensitive to the geo-resolution of exposure. While their corresponding dispersion is reduced by moving towards the smaller resolution. This reduction in tail of dispersion is significantly related to the consideration of spatial correlation. At lower resolution, the distance between the grid cells are higher than finer resolution; subsequently, their corresponding correlation among grid cells are relatively weaker than their counterpart in higher resolution. Thus, the higher variability in ground motion shaking in lower resolution is expected that leads to the higher variability in risk assessment.

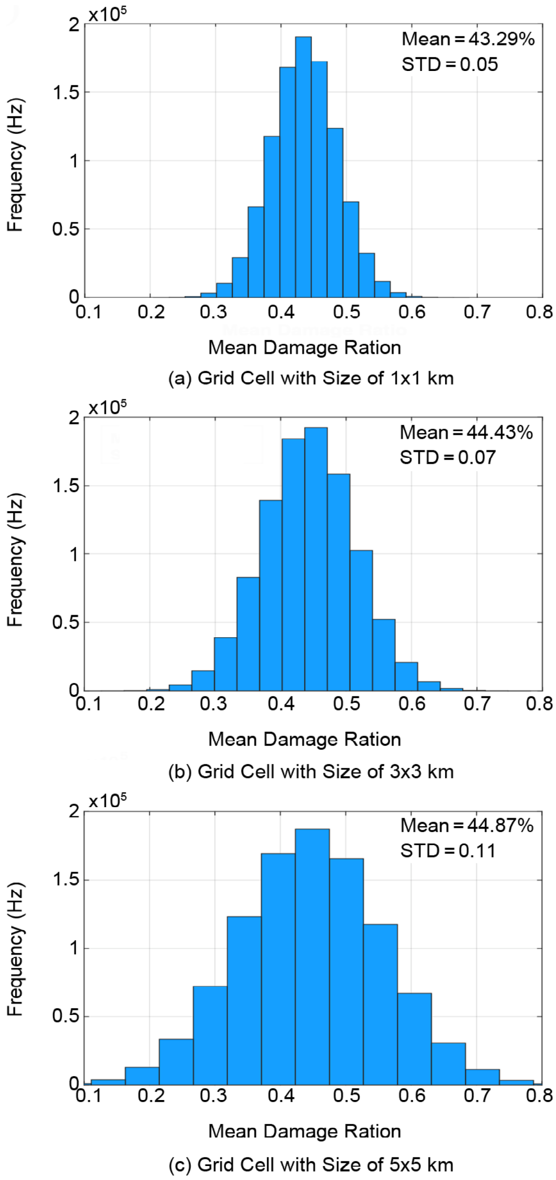

Figure 7. Distribution of mean damage ratio (MDR) from 1,000,000 iterations for the whole of Tehran from the rupture Ray fault in three distinct levels of resolution.

Considering the results, it appears that the total value of damage ratio in a region is almost insensitive to the size of grid cells. While the total standard deviation is reduced in the finer resolution. The question then arises "what is the optimized grid cell for seismic risk assessment?". The answer is entirely depended to the purposes of risk assessment. If the aim of performing the seismic risk analysis in a region is to obtain an overall damage ratio, instead of undergoing significant computation demand by adopting a high resolution exposure model, it is better to lessen the resolution and optimizing the computational efficiency. While the aim of seismic risk in a region is to provide a detailed vulnerability of the region for performing a risk mitigation actions and programs in a region, the computation efficiency should be sacrificed to achieve the most accurate results with lowest uncertainty.

4. Conclusion

This paper looks at sensitivity of seismic losses to the geographic resolution of building exposure model. Exposure model is one of the key components of seismic risk assessment. Generally, exposure models are derived from various sources that are incomplete in format and accuracy. Therefore, the compiled exposure models are associated with epistemic and aleatory uncertainties. Alongside the aforementioned uncertainties, selecting an appropriate geographic size of exposure model is an important issue. This factor directly affects the accuracy and computation efficiency of seismic risk results. From one point of view, implementation of the finer resolution exposure models will result in more accurate outcomes with lower uncertainties. However, refining the resolution will reduce the computational efficiency. In fact, there is a trade-off between accuracy and computational efficiency. The present study shed lights on the sensitivity of seismic risk assessment to the geographic resolution of building exposure model. To this end, the seismic risk assessment was performed for three distinct levels of resolution. Tehran, capital of Iran, is used as case study region. The size of grid cells in the highest resolution is 1 km × 1 km and the coarser resolution is 5 km × 5 km. The results showed that the total value of damage is almost insensitive to the size of grid cells; while a more accurate damage map with lower uncertainty is achieved by refining the resolution. This is largely due to the consideration of spatial correlation. At finer resolution, the distance between the grid cells are lower; subsequently, their corresponding spatial correlation among grid cells are relatively stronger than their counterpart in lower resolution. Thus, the variability in ground motion shaking in higher resolution is smaller that leads to the lower variability in losses. In addition, by moving towards a higher resolution, the uncertainty due to using assumption of uniform distribution of assets in the grid cells and employing the centroid of grid cell as representative of grid for loss estimation will be reduced. In fact, in the refined resolution the geometric centroid of grid cells is closer to the concentration of assets in grid cells.

By consideration of above discussions, this question arises "To what extent expending time and resources in refining the exposure model is reasonable for seismic risk assessments?". The answer is directly depended on the purpose of application of seismic risk assessment. If the aim of seismic risk assessment is to provide an overall estimation of damages in a very large-scale region, implementation of a high spatial resolution of exposure model is not practical. While the purpose of seismic risk assessment is to provide a risk mitigation action or emergency response applications in a region, the expenses of high computational demand should be acknowledged to achieve more accurate results with lower uncertainty.

Acknowledgments

This study is conducted as part of a research program being implemented in the International Institute of Earthquake Engineering and Seismology (IIEES), Tehran, Iran. Its financial and technical supports are fully acknowledged. Additionally, the authors appreciate all those individuals and organizations contributing to the compiling data sets used in the present study, particularly Statistical Center of Iran (SCI) for providing the population databases.

References

1. Firuzi, E., Ansari, A., Amini Hosseini, K., and Rashidabadi, M. (2019) Probabilistic earthquake loss model for residential buildings in Tehran, Iran to quantify annualized earthquake loss. *Bulletin of Earthquake Engineering*, **17**(5), 2383-2406.
2. Firuzi, E., Ansari, A., Amini Hosseini, K., and Karkooti, E. (2020) Developing a customized system for generating near real time ground motion ShakeMap of Iran's earthquakes. *Journal of Earthquake Engineering*, 1-23.
3. Crowley, H. (2006) Earthquake risk assessment: present shortcomings and future directions. *Perspectives on European Earthquake Engineering and Seismology*, 515-532.
4. Organization for Economic Cooperation and Development (OECD) (2012) *Global Modelling of Natural Hazard Risks: Enhancing Existing Capabilities to Address New Challenges, OECD Global Science Forum (Online)*, (Last accessed November 2014).
5. Wieland, M., Pittro, M., Parolai, S., Begaliev, U., Yasunov, P., Tyagunov, S., Moldibekov, B., Saidiy, S., Iiyasov, I., and Abakanov, T. (2015) A multi-scale exposure model for seismic risk assessment in Central Asia. *Seismological Research Letter*, **86**(1), 210-222.
6. Bazzurro, P. and Park, J. (2007, July) The effects of portfolio manipulation on earthquake portfolio loss estimates. In: *Proceedings of the 10th International Conference on Applications of Statistics and Probability in Civil Engineering*, Tokyo, Japan, **31**.
7. Bal, I.E., Bommer, J.J., Stafford, P.E., Crowley, H., and Pinho, R. (2010) The influence of

geographical resolution of urban exposure data in an earthquake loss model for Istanbul. *Earthquake Spectra*, **26**(3), 619-634.

8. Scheingraber, C. and Kaser, M.A. (2019) The impact of portfolio location uncertainty on probabilistic seismic risk analysis. *Risk Analysis*, **39**(3), 695-712.

9. Dabbeek, J., Crowley, H., Silva, V., Weatherill, G., Paul, N., and Nievas, C.I. (2021) Impact of exposure spatial resolution on seismic loss estimates in regional portfolios. *Bulletin of Earthquake Engineering*, **19**(14), 5819-5841.

10. Statistical Centre of Iran (SCI), 1956-2015, *Statistical Centre of Iran, Vice-Presidency for Strategic Planning and Supervision, Tehran, National Census of Population and Housing Technical Reports, Sarshomari 2016 (1395), 2011 (1390), 2006 (1385), 1996 (1375), 1986 (1365), and 1976 (1355): Tehran, SCI, formerly, the Plan and Budget Organization of the Imperial Government of Iran, Statistical Centre*, http://www.amar.org.ir/Default.aspx?tabid=116 (accessed 2018).

11. Motamed, H., Calderon, A., Silva, V., and Costa, C. (2019) Development of a probabilistic earthquake loss model for Iran. *Bulletin of Earthquake Engineering*, **17**(4), 1795-1823.

12. Mansouri, B., Kiani, A., and Amini-Hosseini, K. (2014) A Platform for earthquake risk assessment in Iran case studies: Tehran scenarios and Ahar-Varzeghan earthquake. *Journal of Seismology and Earthquake Engineering*, **16**(1), 51-69.

13. Shahbazi, P., Mansouri, B., Ghafory-Ashtiany, M., and Kaeser, M. (2020) Introducing loss transfer functions to model seismic financial loss: A case study of Iran. *International Journal of Disaster Risk Reduction*, **51**, 101883.

14. Bommer, J.J., Spence, R., Erdik, M., Tabuchi, S., Aydinoglu, N., Booth, E., del Rey, D., and Peterken, O. (2002) Development of an earthquake loss model for Turkish catastrophe insurance. *J. Seismol.*, **6**, 431-446.

15. Berberian, M. (1976) *An Explanatory Note on the First Seismotectonic Map of Iran, a Seismotectonic Review of the Country*. Contribution to the Seismotectonic of Iran (Part III).

16. Japan International Cooperation Agency (JICA) (2000) *Report, The Study on Seismic Microzoning of the Greater Tehran Area in the Islamic Republic of Iran, Final Report, Japan International Cooperation Agency (JICA), Centre for Earthquake and Environmental Studies of Tehran (CEST) Tehran Municipality*, November.

17. Berberian, M. and Robert S.Y. (2017) *Tehran: An earthquake time bomb*.

18. Kalantari, M., Firuzi, E., and Soroushian, S. (2022) *Estimating Annualized Earthquake Loss for Residential Buildings in Tehran, Iran.*

19. Mansouri, B., Ghafory-Ashtiany, M., Amini-Hosseini, K., Nourjou, R., and Mousavi, M. (2010) Building seismic loss model for Tehran. *Earthquake Spectra*, **26**(1), 153-168.

20. Hessami, K., Jamali, F., and Tabassi, H. (2003) *Active Fault Maps of Iran*. Seismotectonic Department, Seismology Research Center, Institute of Earthquake Engineering and Seismology (IIEES), Iran.

21. Moinfar, A., Mahdavian, A., and Maleki, E. (1994) Historical and instrumental earthquake data collection of Iran. *Publication Iranian Culture*. Affairs Inst, Tehran, p.446

22. Pagani, M., Monelli, D., Weatherill, G., Danciu, L., Crowley, H., Silva, V., ... and Vigano, D. (2014) OpenQuake engine: an open hazard (and risk) software for the global earthquake model. *Seismological Research Letters*, **85**(3), 692-702.

23. Wells, D.L. and Coppersmith, K.J. (1994) New empirical relationships among magnitude, rupture length, rupture width, rupture area, and surface displacement. *Bull. Seism. Soc. Am.*, **84**, 974-1002.

24. Kale, O., Akkar, S., Ansari, A., and Hamzehloo, H. (2015) A ground motion predictive model for Iran and Turkey for horizontal PGA, PGV,

and 5% Damped response spectrum: investigation of possible regional effects. *Bulletin of the Seismological Society of America*, **105**(2A), 963-980.

25. Kotha, S.R., Bindi, D., and Cotton, F. (2016) Partially non-ergodic region specific GMPE for Europe and middle-east. *Bulletin of Earthquake Engineering*, **14**(4), 1245-1263.

26. Akkar, S. and Bommer, J.J. (2010) Empirical equations for the prediction of PGA, PGV, and spectral accelerations in Europe, the Mediterranean region, and the middle East. *Seismological Research Letters*, **81**(2), 195-206.

27. Zhao, J.X., Zhang, J., Asano, A., Ohno, Y., Oouchi, T., Takahashi, T., ... , and Fukushima, Y. (2006) Attenuation relations of strong ground motion in Japan using site classification based on predominant period. *Bulletin of the Seismological Society of America*, **96**(3), 898-913.

28. Idriss, I.M. (2014) An NGA-west2 empirical model for estimating the horizontal spectral values generated by shallow crustal earthquakes. *Earthquake Spectra*, **30**(3), 1155-1177.

29. Weatherill, G.A., Silva, V., Crowley, H., and Bazzurro, P. (2015) Exploring the impact of spatial correlations and uncertainties for portfolio analysis in probabilistic seismic loss estimation. *Bulletin of Earthquake Engineering*, **13**(4), 957-981.

30. Verros, S.A., Wald, D.J., Worden, C.B., Hearne, M., and Ganesh, M. (2017) Computing spatial correlation of ground motion intensities for shakemap. *Computers and Geosciences*, **99**, 145-154.

31. Zafarani, H., Ghafoori, S.M.M., and Adlaparvar, M.R. (2022) Spatial correlation of peak ground motions and pseudo spectral acceleration based on the Iranian multievent datasets. *Journal of Earthquake Engineering*, **26**(12), 6042-6062.

32. Zafarani, H., Noorzad, A., Ansari, A., and Bargi, K. (2009) Stochastic modeling of Iranian earthquakes and estimation of ground motion for future earthquakes in Greater Tehran. *Soil Dynamics and Earthquake Engineering*, **29**(4), 722-741.

33. Fallah Tafti, M., Amini Hosseini, K., and Mansouri, B. (2020) Generation of new fragility curves for common types of buildings in Iran. *Bulletin of Earthquake Engineering*, **18**(7), 3079-3099.

34. Bastami, M., Abbasnejadfard, M., Motamed, H., Ansari, A., and Garakaninezhad, A. (2022) Development of hybrid earthquake vulnerability functions for typical residential buildings in Iran. *International Journal of Disaster Risk Reduction*, 103087.

35. Silva, V., Crowley, H., Yepes, C., and Pinho, R., (2014), Presentation of the OpenQuake engine, an open source software for seismic hazard and risk assessment. *Tenth U.S. National Conf. on Earthquake Engineering*, Anchorage, Alaska.

36. Whitman, R.V., Anagnos, T., Kircher, C.A., Lagorio, H.J., Lawson, R.S., and Schneider, P. (1997) Development of a national earthquake loss estimation methodology. *Earthquake Spectra*, **13**, 643-661.